ASSESSMENT OF DYNAMIC RESPONSES OF 5 MW FLOATING OFFSHORE WIND TURBINE PLATFORMS IN INTERMEDIATE WATER DEPTH

Joshua Cutler, *School of Engineering, Liverpool John Moores University, Liverpool, L3 3AF, UK*
Musa Bashir*, *School of Engineering, Liverpool John Moores University, Liverpool, L3 3AF, UK*
Yang Yang, *School of Engineering, Liverpool John Moores University, Liverpool, L3 3AF, UK*
Jin Wang, *Faculty of Maritime and Transportation, Ningbo University, Ningbo, 315211, P.R. China*
Sean Loughney, *School of Engineering, Liverpool John Moores University, Liverpool, L3 3AF, UK*

ABSTRACT

This paper presents a comparative numerical study on the dynamic responses of three Floating Offshore Wind Turbine (FOWT) concepts operating, in 150m of water. The study examined three concepts (OC3-Hywind spar, ITI Energy barge and a novel catamaran FOWT) all supporting the NREL 5MW reference wind turbine. The three concepts were modelled using OpenFAST and ANSYS AQWA numerical tools coupled via a DLL, namely F2A, in order to conduct efficient aero-hydro-servo-elastic simulations. F2A has the advantage of combining the superiority of AQWA in predicting hydrodynamic loads and mooring tensions with the aerodynamic capabilities of OpenFAST to perform fully coupled simulations. Assessment of the FOWTs' dynamic behaviors and performance is carried out following the prediction of dynamic responses. A comparison of the rigid body motion responses of the fully coupled models, including mooring line tensions, is presented. More specifically, performance indicators of the wind turbines including dynamic responses, stability and power production under operational conditions are presented. The results and conclusions of this paper can provide greater insight into the behavior of different FOWT concepts operating under different environmental conditions as well as resolve the fundamental design trade-offs between different FOWT concepts.

1. INTRODUCTION

For water depths greater than 60 m, Floating Offshore Wind Turbines (FOWTs) are recognised as the most cost-effective solution to harness offshore wind energy. Approximately 80% of the world's offshore wind resource potential is located in waters deeper than 60 m [1]. FOWTs will create new markets and unlock acres of marine space where depth and poor bathymetry previously constrained fixed-bottom offshore wind farm development.

Over the last decade, numerous FOWT projects have been completed, see **Figure 1**. In 2015, Equinor expanded the world's first FOWT pilot project into the world's first fully operational floating offshore wind farm, consisting of five 6 MW spar-type FOWTs [2]. In 2018, Ideol installed demonstrators of its Damping Pool barge-type FOWT concept, in the waters off the coasts of France [3] and Japan [4]. At the end of 2019, Principle Power completed the WindFloat Atlantic project [5], where three 8.4 MW semisubmersible-type FOWTs were connected to the Portuguese electricity grid. These are currently the largest FOWTs in the world and the power generated could supply up to 60,000 users each year.

FOWTs can be classified in terms of how they achieve hydrostatic stability in pitch and roll [6] [7]:

- ballast stabilized (low centre of gravity), e.g. spars
- mooring stabilized e.g. tension leg platforms (TLP)
- buoyancy stabilized e.g. semisubmersible and barge

Each type of FOWT has its own unique advantages and disadvantages. Spars are a promising option because of structural simplicity [8] and excellent hydrodynamic stability. However, the primary characteristic of a spar, its draft, is also its limitation, as they cannot be deployed in shallow waters [9].

Barges present building, deployment, anchoring, site independence and decommissioning advantages, but are limited in terms of platform-pitch stability, wave sensitivity and control complexity [10].

Semisubmersibles can be deployed in a variety of water depths and have superior hydrodynamic stability. However, the design of semisubmersibles is more challenging due to the complex dynamic

responses induced by combined wind-wave loads. The heave response is a primary concern of semisubmersible FOWTs [11]. Also, the construction of semisubmersibles is more complex compared to the other types.

TLP FOWTs have great cost potential and very good heave and angular motions, but are without the lack of full-scale testing; both the costs and the risks are still somewhat unknown. Three major hurdles for TLPs include the complexity and cost of the mooring installation, the change in tendon tension due to tidal variations, and the structural frequency coupling between the tower and the mooring system [12].

Over the last decade, a small number of researchers have conducted studies in a bid to resolve preliminary design trade-offs among different FOWT concepts.

A dynamic response analysis of three FOWT concepts was carried out in [6]. A TLP, spar and barge was assessed and compared. Comparisons were based on ultimate loads, fatigue loads and instabilities. The analysis discovered instabilities in all systems and that the barge was susceptible to excessive platform-pitching in extreme waves.

[13] analysed the dynamic responses of six FOWT concepts. Three concepts were identical to the concepts assessed in [6]. The other three are generic systems created for a demonstration project and include another TLP, a semisubmersible and spar. The TLP is of a different design compared to the TLP modelled in the previous study. The design of the spar remained constant but was modelled at a different water depth. Despite the two different TLP designs, the analysis found that their response was fairly similar. It was identified that the method for stabilizing the floating system is more influential on the dynamics of the system as opposed to the details of the design. The effect of water depth on the OC3-Hywind system did not have a significant effect on the system dynamics.

[14] carried out 1/50th scale wind/wave basin model tests of three concepts. Experimental performance results were discussed and compared for a number of wind-wave environments, with emphasis placed on global motions, flexible tower dynamics and mooring system response.

[15] investigated the dynamical characteristics of a spar and semisubmersible by model testing. A series of comparisons were made based on the experimental results. It was found that the dynamic behaviours of the two FOWTs had some similarities and some significant differences. The spar was more sensitive to wind loading and had larger amplitudes of platform motion in wind only cases. By contrast, the semisubmersible was more sensitive to wave loading, particularly for second order difference-frequency wave loading.

Even though researchers have quantified to some extent, the impact of platform type on turbine loads and design, no definitive conclusion can be drawn on which platform type is the best.

Ultimately, the end goal is utility-scale production of FOWTs. Barge-type platforms have advantages in fabrication, deployment and installation. The

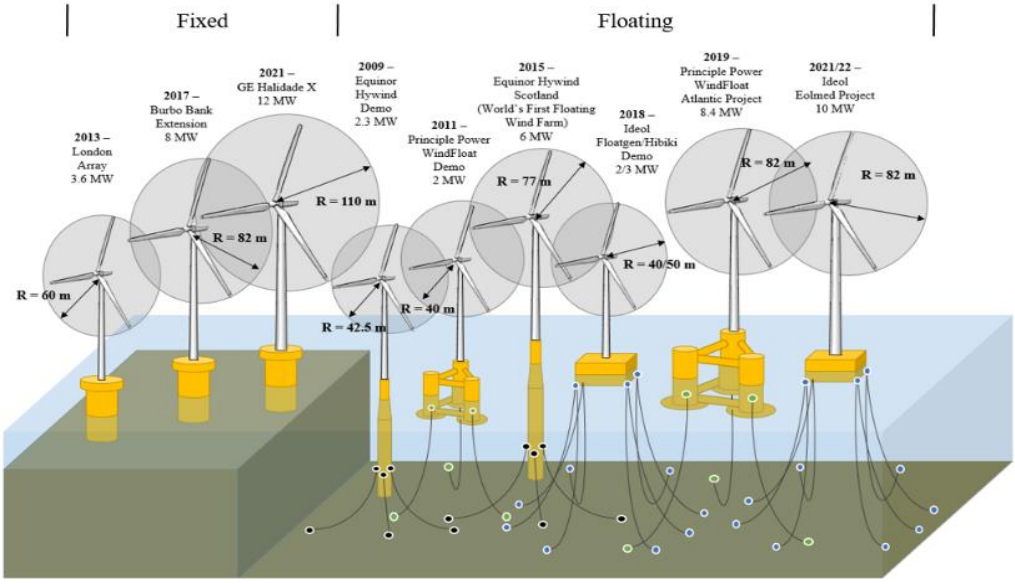

Fig 1. The growth in size and output capacity of offshore wind turbines over time.

simple geometry allows for straightforward construction and the wind turbine can be mounted onto the floating platform at quayside before tugging the entire assembly offshore, eliminating the need for specialist vessels. Such factors mean barge-type FOWTs have lower overall costs compared to the others. However, pitch stability is the major limitation of this platform type. Spars are another platform type showing strong potential for mass production, except depth is a limiting factor. To improve on the pitch stability of barge-type platforms whilst maintaining simplicity in design, a novel catamaran platform is introduced.
Therefore, this paper analyses the dynamic behaviours of three FOWTs in intermediate water depth: barge, spar, and catamaran. The outcomes of this work hope to provide greater insight into the behaviour of different FOWT concepts operating under different environmental conditions as well as contribute to resolving the fundamental design trade-offs between different FOWT concepts.

2. MODEL DESCRIPTION

The FOWT systems studied in this work are described herein. Each FOWT is composed of the following parts: (1) floating platform, (2) tower, (3) rotor and nacelle assembly, and (4) mooring system. All three floating platforms support the NREL 5 MW reference wind turbine which is detailed in Table 1. The wind turbine is a conventional three-bladed, upwind variable-speed wind turbine.

Table 1. Properties of NREL 5 MW Reference Wind Turbine.

Parameter (Units)	Value
Rated Power (MW)	5
Rotor & hub diameter (m)	126 & 3
Cut-in, rated, cut-out wind speed (ms^{-1})	3, 11.4, 25
Hub height (from the bottom of the tower) (m)	90
CM location (from bottom of the tower) (m)	64
Rotor mass (kg)	110,000
Nacelle mass (kg)	240,000
Tower mass (kg)	347,460
Total mass (including tower) (kg)	697,460

Three floating platforms are modelled in this study which include a spar, a barge and a catamaran. The platforms are depicted in **Fig. 2** and mooring system arrangements in **Fig. 3**. The properties of the floating platforms and respective mooring systems are presented in **Table 2**.

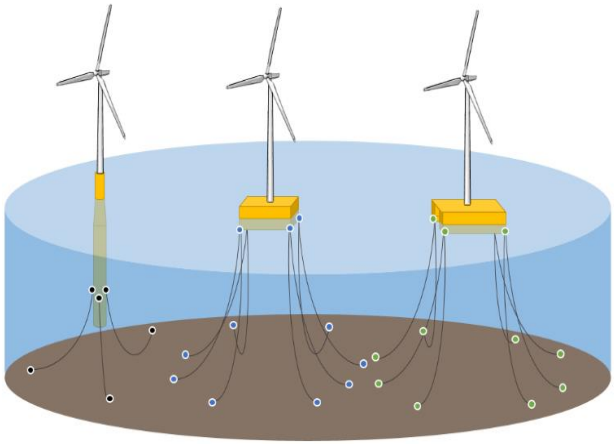

Figure 2. Three FOWT concepts under investigation: spar (left), barge (centre), catamaran(right).

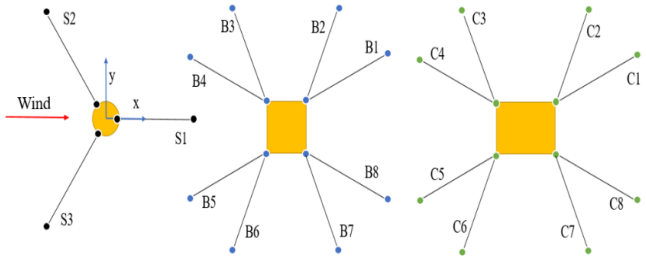

Figure 3. Mooring system configuration of each FOWT under investigation: spar (left), barge (centre), catamaran(right).

The spar FOWT has been previously defined in the Phase IV of the OC3 project [16]. The configuration of the OC3-Hywind spar features a deeply drafted, slender spar buoy, and the floating system is held in position by three mooring lines. One of the cables is directed along the positive x-axis in the x-z plane, and the other two remaining lines are distributed uniformly (120°) around the platform. The water depth in this study is 150 m which differs to previous work. Thus, slight modifications of the mooring system are required.
The barge-type FOWT is commonly referred to as the ITI Energy Barge, a preliminary barge concept developed by the Universities of Glasgow and Strathclyde, and ITI energy. More specifications can be seen in [17]. To prevent it from drifting, the floating platform is moored by a system of eight slack, catenary lines. Two mooring lines join at each corner of the bottom of the barge such that they are 45° apart at the corner.

The catamaran FOWT is based on a typical catamaran vessel comprised of a large deck mounted atop two equally spaced demi-hulls. The wind turbine is situated in the middle of the platform so that the tower centreline and platform centreline align and pass through the origin (0,0). Similarly, to the barge-type FOWT, eight slack, catenary lines keep the platform in position.

Table 2. Platform and Mooring System Properties of the Three FOWT Concepts.

	OC3 Hywind Spar	ITI Energy Barge	Catamaran
Diameter or width x length (m)	6.5 (above taper), 9.4 (below taper)	40 x 40	45 x 60, (LOA = 77.3)
Space between demi-hulls (m)	-	-	25
Draft (m)	120	4	4
Elevation to platform top (tower base) above SWL	10	6	6
Total volume (m^3)	8,361	16,000	15,684
Water displacement (m^3)	8,029	6,400	5,480
Mass (kg)	7,466,330	5,452,000	4,901,080
CM location (m)	(0, 0, -89.916)	(0, 0, -0.282)	(0, 0, 1.51)
Roll inertia about CM (kg m^2)	4,229,230,000	726,900,000	4,672,683,194
Pitch inertia about CM (kg m^2)	4,229,230,000	726,900,000	6,800,310,371
Yaw inertia about CM (kg m^2)	164,230,000	1,454,000,000	11,190,569,096
Number of mooring lines	3	8	8
Depth to fairleads & anchors (m)	70 & 150	4 & 150	-4 & 150
Radius to fairleads & anchors (m)	5.2 & 274.6	28.28 & 423.4	42.436 & 429.095
Section length (m)	287	473.4	473.312
Mooring line diameter (m)	0.09	0.0809	0.0809
Line mass density (kg m^{-1})	173	130.4	130.4
Line extensional stiffness, EA (N)	384,200,000	589,000,000	589,000,000

3. FAST2AQWA TOOL

To accurately predict the dynamic responses of the three FOWT concepts, subjected to a range of operational environmental conditions, a new aero-hydro-servo-elastic coupled tool based on the commercial hydrodynamic analysis software tool AQWA [18] and FAST [19] is adopted in this study. Since the release of this novel coupling framework, FAST has transitioned to OpenFAST. OpenFAST [20] is an open-source version of FAST, where FAST is the framework that couples computational modules for aerodynamics, hydrodynamics (offshore structures), control and electrical system dynamics, and structural dynamics to enable fully coupled nonlinear aero-hydro-servo-elastic simulation in the time domain. The new tool used in this analysis replaces the hydrodynamic module, known as HydroDyn, used to calculate the hydrodynamic loads of a FOWT in FAST with the far superior predictive capabilities of AQWA. The aero-servo-elastic simulation capabilities of FAST are implemented within AQWA via a coupling framework referred to as FAST2AQWA (F2A). The coupling between AQWA and FAST is achieved via the user_force64.dll which is a built-in Dynamic Link Library (DLL) of AQWA for external force calculation. This is illustrated by a flowchart presented in **Fig. 4** [21].

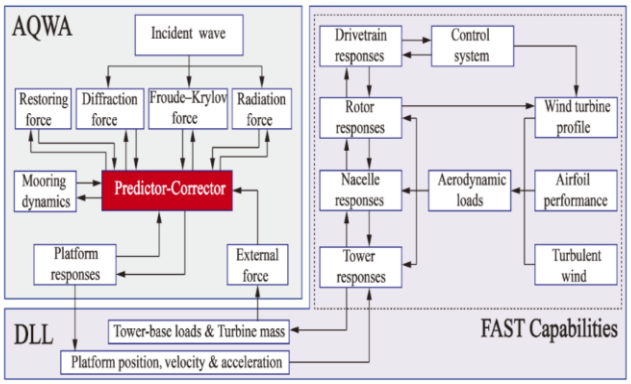

Figure 4. Flowchart of F2A [21].

It can be seen in **Fig. 4** that the dynamic responses of a FOWT are predicted in different modules. Similarly, to FAST, F2A is the framework that couples all the computational modules together. More explicitly, the upper structures of the wind turbine (tower, rotor and nacelle) are modelled in FAST and the dynamic responses are predicted within the DLL using the platform kinematics

obtained in AQWA. However, before being passed into the DLL these terms are transformed from the inertial coordinate system to the local coordinate system of the platform. The reason for this is because FAST corrects the kinematics of the upper structures based on the platform responses that are referred to its local coordinate system, thus, a transformation is needed as the platform responses predicted by AQWA are referred to its inertial coordinate system. Subsequently, the tower-base loads are calculated by the FAST subroutines. The lower structure, which consists of the platform and mooring lines, is modelled in AQWA. The dynamic responses are calculated in AQWA by solving the equation of motion of the platform considering the calculated tower-base loads as an external force. Another appropriate transformation is applied to the external force referring it back to the inertial coordinate system. The governing equation of motion of the platform is defined in **Eq. 1.**

$$(\boldsymbol{M}+\boldsymbol{A})\ddot{x}+(\boldsymbol{B}_{ext}+\boldsymbol{B}_{Pot})\dot{x}+\boldsymbol{B}_2\dot{x}|\dot{x}|+\int_0^t \boldsymbol{h}(t-\tau)\dot{x}(\tau)d\tau+\boldsymbol{C}x=\boldsymbol{F}_{ext} \quad [1]$$

where $\boldsymbol{M}$ is the inertial mass matrix, $\boldsymbol{A}$ is the added mass matrix, and x, $\dot{x}$, $\ddot{x}$ are the unknown displacement, velocity, and acceleration vectors of the platform, respectively, for each degree of freedom. Similarly, $\boldsymbol{B}_{ext}$ and $\boldsymbol{B}_2$ are the damping coefficients matrix related to viscous (quadratic) damping typically obtained from model tests, $\boldsymbol{B}_{Pot}$ is the radiation or potential (linear) damping matrix, while $\boldsymbol{C}$ is the stiffness matrix composed by hydrostatic and the mooring line restoring forces. Matrix $\boldsymbol{A}$ and $\boldsymbol{B}_{Pot}$ can be computed by a numerical code based on the potential theory, in this case AQWA, which in turn can provide the total external force vector denoted by $\boldsymbol{F}_{ext}$. In the case of an irregular wave spectrum, the fluid memory has an important impact on the floating body dynamics. This fluid memory effect is captured by the convolution integral formulation based upon the Cummins equation. Furthermore, $\boldsymbol{h}(t)$ is the radiation impulse function matrix used to examine the radiation memory effects as defined in **Eq. 2**.

$$\boldsymbol{h}(t)=\frac{2}{\pi}\int_0^{\infty}\boldsymbol{B}_{Pot}(\omega)\cos(\omega t)\,d\omega, \quad [2]$$

where $\boldsymbol{B}_{Pot}(\omega)$ is the radiation damping corresponding to the wave frequency of ω. For more information on the F2A coupling framework and coordinate system transformations refer to [22].

4. LOAD CASES, ENVIRONMENTAL CONDITIONS AND SIMULATION

Based on the met-ocean data of a specific site situated off the north coast of Scotland, five Load Cases (LCs) are defined in **Table 3.** The LCs represent a range of potential environment conditions within the NREL 5MW reference turbine operation wind speed range. U_w is the mean wind speed at hub-height, H_s is the significant wave height and T_p is the spectral peak period. The three-dimensional turbulent wind fields were generated using NREL's TurbSim program [23] according to the Kaimal turbulence model for IEC Class C. The kinematics of the irregular waves are generated based on the P-M spectrum in AQWA. In this study, both wind and waves are unidirectional and aligned with x-axis for all three FOWTs.

Table 3. Load Cases.

LC	U_w [m/s]	H_s [m]	T_p [s]
1	4	1.6146	3.4985
2	8	1.8037	4.2657
3	11.4	2.1155	5.2555
4	18	2.9585	7.1203
5	25	4.0257	8.8897

For each simulation, the overall simulation length is 4,600 s and the first 1,000 s is removed to negate any transient effects interfering with the final statistical results. The hydrodynamic characteristics and dynamic responses of the three FOWT concepts are examined for each load case after predictions are made using F2A.

5. ASSESSMENT OF DYNAMIC RESPONSES

5.1 FREE DECAY ANALYSIS

A free decay analysis was conducted for each concept in all six degrees of freedom. The natural period and frequency of the relevant platform in each rigid body mode is presented in **Table 4**.

Table 4. Natural periods and frequencies of the FOWT platforms.

	Surge	Sway	Heave	Roll	Pitch	Yaw
Spar						
Period/(s)	82.2	82.2	30.4	30.1	30.1	6.1
Frequency/(Hz)	0.012	0.012	0.033	0.033	0.033	0.164
Barge						
Period/(s)	137.7	137.7	7.1	11.8	11.8	52.5
Frequency/(Hz)	0.007	0.007	0.141	0.085	0.085	0.019
Catamaran						
Period/(s)	121.6	157.1	5.4	10.6	9.8	109.5
Frequency/(Hz)	0.008	0.006	0.185	0.094	0.102	0.009

5.2 PLATFORM MOTIONS

The statistical results of the platform motions of the three concepts are presented in **Table 5**. For all LCs, the spar has the smallest surge response, owing to its small water plane area. However, floating platforms that achieve hydrostatic stability through buoyancy, like the barge and catamaran, require large water plane areas, and typically have large geometric volumes in the vicinity of the water's surface where the highest concentration of wave energy exists. In contrast, the surge response of the barge and catamaran are much higher and have a greater variation compared to the spar. The highest mean surge response for all three platforms was observed in LC 3. This corresponds to the rated wind speed condition. A wind turbine operating at rated wind speed produces maximum rotor thrust (approx. 800kN for 5 MW wind turbine), which significantly contributes to the surge response. Under LC 5, all three platforms had their greatest maximum surge response. Compared to the spar, the barge and catamaran had approximately two and three times the surge displacement, respectively. It can be inferred from that the barge and catamaran are more sensitive to wave loading compared to the spar because of the responses observed by these platforms in the direction of wave propagation.

Buoyancy-stabilised platforms tend to have minimal heave responses. The hydrostatic restoring force provided by buoyancy as a result of the large water plane area restricts the vertical motion. Conversely, the water plane area of the spar is small, as such the restoring forces are not

Table 5. Statistical platform responses of the three FOWT concepts (1000 – 4600 s).

		Surge/m			Heave/m			Pitch/ °		
LC	Type	Spar	Barge	Cat	Spar	Barge	Cat	Spar	Barge	Cat
	Max	**4.747**	16.35	16.96	0.708	0.300	**0.066**	1.658	1.025	**0.314**
1	Mean	**2.620**	8.490	8.343	0.650	**0.123**	-0.125	0.917	0.328	**0.067**
	Std.dev	**0.733**	3.198	2.734	**0.023**	0.059	0.059	0.251	0.179	**0.080**
	Max	**12.52**	33.35	34.68	0.655	0.645	**0.456**	4.146	2.153	**1.581**
2	Mean	**8.168**	22.32	22.25	0.436	**0.115**	**-0.115**	2.865	1.094	**0.295**
	Std.dev	**1.381**	3.674	3.809	**0.085**	0.156	0.114	0.432	**0.226**	0.312
	Max	**18.73**	45.52	48.14	0.756	1.149	**0.410**	7.456	3.826	**2.936**
3	Mean	**12.44**	29.29	27.18	0.132	**0.108**	-0.143	4.452	1.726	**0.370**
	Std.dev	**2.240**	7.050	11.31	0.228	0.308	**0.151**	0.969	**0.545**	0.712
	Max	**12.99**	30.08	44.41	**1.096**	2.148	1.720	6.189	**4.243**	8.519
4	Mean	**7.168**	19.30	21.92	0.500	**0.118**	-0.134	2.561	0.997	**0.200**
	Std.dev	**1.916**	4.298	8.046	**0.158**	0.593	0.398	1.168	**1.026**	2.492
	Max	**21.89**	37.19	50.03	4.058	3.352	**2.727**	14.330	**12.190**	12.770
5	Mean	**4.710**	8.583	20.60	0.570	0.122	**-0.104**	1.785	0.862	**0.179**
	Std.dev	**6.157**	11.53	10.78	0.775	0.895	**0.733**	4.370	**3.775**	4.046

large enough to limit the heave motion. However, as the spar has a large draft, vertical forces acting on the structure are negligible, and the heave response is insignificant. All three platforms show good response in heave for all five LCs.

The elongated body of the catamaran platform provides a greater restoring moment about the y-axis compared to the other two platforms, which improves platform stability against rotational motion about the y-axis (pitch). For all LCs, the catamaran platform has the lowest mean pitch response of the three platforms. On the contrary, for all five cases the spar platform has the highest mean pitch response which suggests that the spar is more sensitive to aerodynamic loading than the other two platforms. Similarly, the highest mean pitch response for the three platforms is observed in LC 3, the rated wind speed condition.

5.3 MOORING LINE RESPONSES

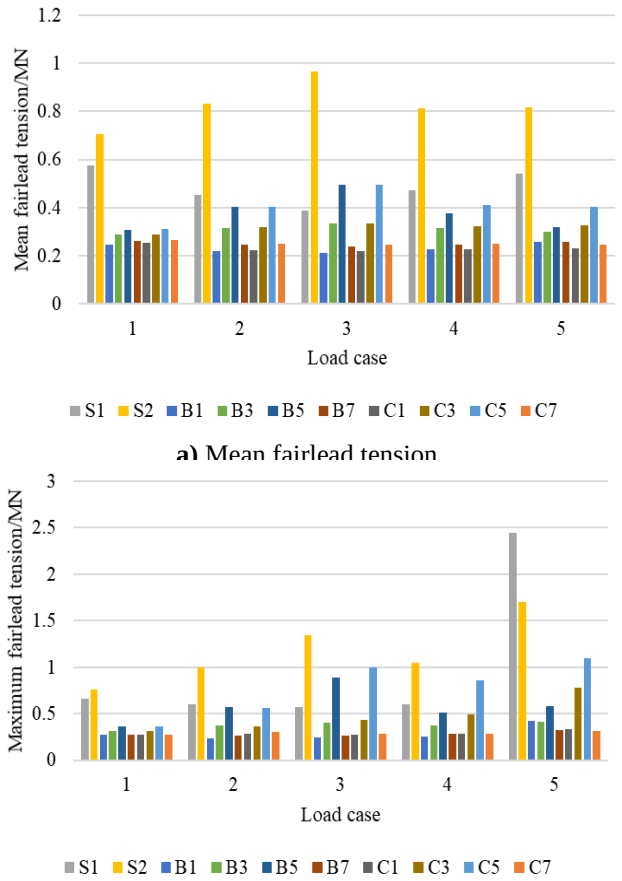

b) Maximum fairlead tension.

Figure 7. Tension in the mooring lines of the three FOWTs (S1 = spar line 1, B1 = barge line 1, C1 = catamaran line 1).

Figure 7.a) and **b)** present the mean and maximum fairlead tensions of the three FOWTs. Each mooring system configuration is symmetrical which means only certain mooring lines need analysis. Therefore, two mooring lines of the spar mooring system (S1, S2) and four mooring lines of the barge (B1, B3, B5, B7) and catamaran (C1, C3, C5, C7) mooring systems are selected. The spar mooring system is made up of three mooring lines in total to keep the platform in position, whereas the other two mooring systems use eight. Therefore, the moorings lines tensions of the spar mooring system will have a greater mean tension compared to the barge and catamaran mooring systems. This is evident in **Fig. 7.a**.

Moreover, as a result of the incident waves, prevailing wind and rotor thrust all acting or travelling downwind, the mooring lines upwind of the origin will exhibit the greatest tension. This is because the environmental phenomena cause the platform to drift downwind, as it does, the mooring lines upwind will stretch in order to prevent drifting whilst the mooring lines downwind will slack. The barge and catamaran mooring lines have similar mean tensions under all LCs, except for mooring line C5 in LCs 4 and 5 where C5 is higher than B5. Under these two LCs, the maximum tension of mooring line C5 is approximately 1.6 times the tension of B5 under LC4 and 2 times the tension under LC 5. This can be explained by the greater surge response of the catamaran platform under these two LCs. Therefore, the mean tension of mooring line C5 will be higher than the equivalent mooring line of the barge mooring system.

5.4 POWER PRODUCTION

The power generation of the three FOWTs for all examined LCs are presented in **Figure 8**. All three power curves are very alike. The results infer that the floating platform type used to support the wind turbine in intermediate water depth, under the specified operational conditions, has little effect on the power generated by the wind turbine.

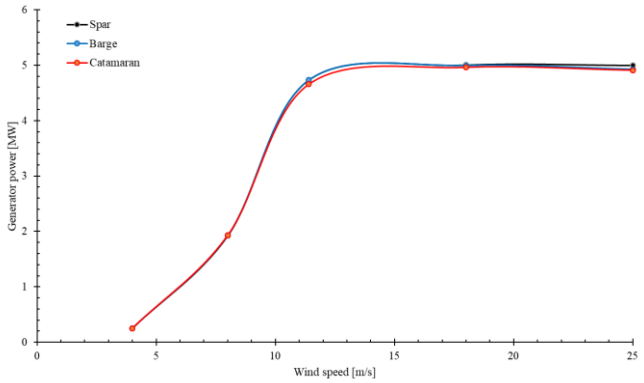

Figure 8. Power curves of each FOWT.

5.5 UPPER STRUCTURE RESPONSES

In **Figures 9, 10 & 11** the rotor thrust, out-of-plane blade-tip deflection and fore-aft tower-base bending moment of the three FOWTs are plotted. All three structural performance indicators follow a similar trend due to being affected directly or indirectly by the incoming wind. The rotor thrust is the axial force applied by the wind on the rotor and it is the dominant load acting on each FOWT. The out-of-plane blade-tip deflection is the result of the force exerted by the wind on the turbine blades. The fore-aft tower-base bending moment is caused by the rotor thrust and has the most prominent influence on stress at the tower base.

It can be observed that the peak thrust acting on all three rotors occurs at rated wind speed (LC 3). This is also true for the peak fore-aft tower-base bending moment and blade deflection. Comparing the three FOWTs, for all LCs, the spar platform has the highest rotor thrust while the catamaran platform that has the lowest. For LC 3, the spar, barge and catamaran FOWTs have an approximate rotor thrust of 800 kN, 750 kN, and 700 kN, respectively. This means compared to the catamaran, the spar and barge have a 14 % and 7 % larger rotor thrust, respectively.

Under the same LC, the fore-aft tower-base bending moment of the spar, barge and catamaran is 78 MN·m, 64 MN·m and 52 MN·m, respectively. The fore-aft tower-base bending moment in the spar is 50 % larger compared to the catamaran and 22 % compared to the barge.

Blade deflection does not have a sizeable impact on power output unless the severity is great enough as to reduce the swept area. The difference between the catamaran and spar peak out-of-plane blade-tip deflection is 6.7%. This suggests the platform type does not significantly influence the out-of-plane blade-tip deflection compared to rotor thrust and the fore-aft tower-base bending moment. Equally, as a result of the spar surge displacement in LC 5, the difference between the blade-tip deflection of the spar and barge is 54 % which is the greatest difference out of all LCs between these two platforms. Still, the magnitude of the out-of-plane blade-tip deflection under LC 5 is the smallest for all LCs.

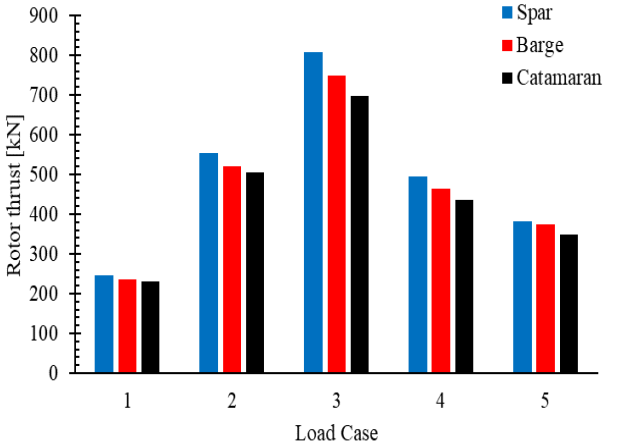

Figure 9. Comparison of rotor thrust.

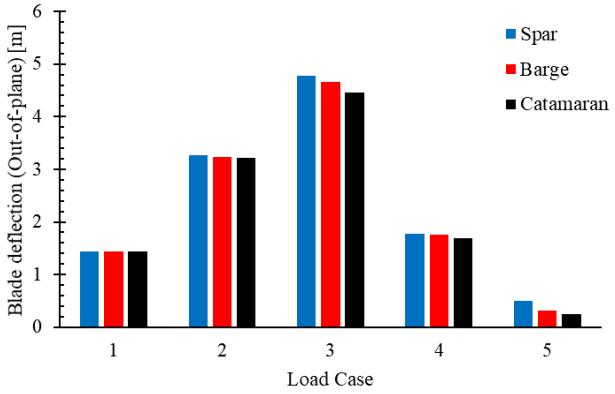

Figure 10. Comparison of blade deflection.

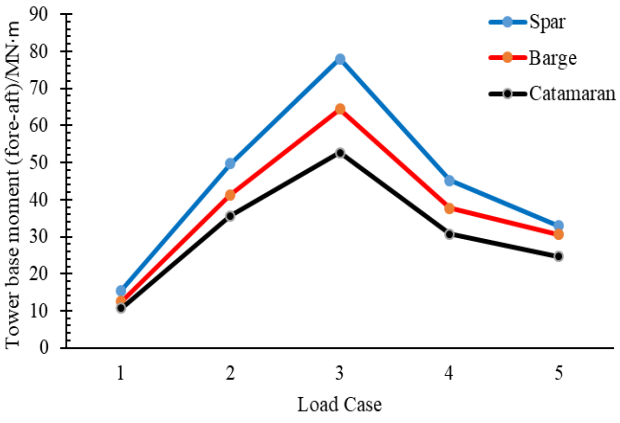

Figure 11. Comparison of fore-aft tower-base bending moment

6. CONCLUSIONS

The dynamic responses of three FOWT concepts, including a novel catamaran FOWT, operating in intermediate water depth are assessed and compared. The three FOWTs are modelled using OpenFAST and ANSYS AQWA numerical tools coupled via a DLL, namely F2A, in order to conduct efficient aero-hydro-servo-elastic simulations. The main conclusions of this study are as follows:

- The spar has the smallest surge response whilst the catamaran has the largest for all LCs. The highest mean surge response for all three platforms was observed under LC 3 which corresponds to rated wind speed condition. The maximum surge response for all three platforms was observed under LC 5. The barge and catamaran FOWTs are more sensitive to wave loading compared to the spar.
- All three platforms showed a limited heave response. The barge and catamaran platforms have a large water plane areas and therefore excellent hydrostatic stiffness against vertical motion. The spar's large draft means vertical forces acting on the structure are negligible, and the heave response is insignificant.
- The catamaran has the lowest average pitch response for all LCs, a significant finding, whilst the spar has the highest average pitch response. The spar FOWT is more sensitive to aerodynamic loading compared to the other two FOWTs. Similarly, to the surge response, the highest mean pitch response was observed under rated conditions.
- The floating platform type has inconsequential effects on the power generation of the wind turbine; thus, the catamaran floating platform can be considered a promising option for the specified environmental conditions in this respect.
- Under LC 3, compared to the catamaran, there is a difference in rotor thrust of 14 % and & 7% for the spar and barge, respectively. Similarly, compared to the catamaran, there is a difference in the fore-aft tower-base bending moment of 50 % and 22 % for the spar and barge, respectively.

This study has showed that a catamaran floating platform is the more effective solution to support a 5 MW wind turbine over the spar and barge platforms. Not only can the generated power produced by the turbine match the conventional floating platforms, but the catamaran platform also provides great stability which ultimately leads to reductions, some considerable, of key performance indicators. The surge response of a catamaran type floating platform is one area for future work.

ACKNOWLEDGEMENTS

The authors would like to acknowledge the financial support from the European Regional Development Fund (ERDF), Interreg Atlantic Area (grant number: EAPA_344/2016). Financial support from Liverpool John Moores University is also thanked.

REFERENCES

[1] Equinor, 'The future of offshore wind is afloat'. https://www.equinor.com/en/what-we-do/floating-wind.html (accessed Sep. 22, 2021).

[2] Equinor, 'Hywind Scotland'. https://www.equinor.com/en/what-we-do/floating-wind/hywind-scotland.html (accessed Jul. 14, 2021).

[3] Ideol, 'FLOATGEN'. https://floatgen.eu/ (accessed Jul. 14, 2021).

[4] Ideol, 'HIBIKI - Floating wind turbine solution | Japan offshore wind'. https://www.bw-ideol.com/en/japanese-demonstrator (accessed Jul. 14, 2021).

[5] Principle Power, 'WindFloat'. https://www.principlepowerinc.com/en/windfloat (accessed Aug. 16, 2021).

[6] J. Jonkman and D. Matha, 'Dynamics of offshore floating wind turbines-analysis of three concepts', *Wind Energy*, vol. 14, no. 4, pp. 557–569, 2011, doi: 10.1002/we.442.

[7] K. P. Thiagarajan and H. J. Dagher, 'A review of floating platform concepts for offshore wind energy generation', *J. Offshore Mech. Arct. Eng.*, vol. 136, no. 2,

pp. 1–6, 2014, doi: 10.1115/1.4026607.
[8] L. Meng *et al.*, ‘Dynamic Response of 6MW Spar Type Floating Offshore Wind Turbine by Experiment and Numerical Analyses’, *China Ocean Eng.*, vol. 34, no. 5, pp. 608–620, 2020, doi: 10.1007/s13344-020-0055-z.
[9] Z. Zheng, J. Chen, H. Liang, Y. Zhao, and Y. Shao, ‘Hydrodynamic responses of a 6 MW spar-type floating offshore wind turbine in regular waves and uniform current’, *Fluids*, vol. 5, no. 4, pp. 1–28, 2020, doi: 10.3390/fluids5040187.
[10] J. Olondriz, I. Elorza, J. Jugo, S. Alonso-Quesada, and A. Pujana-Arrese, ‘An advanced control technique for floating offshore wind turbines based on more compact barge platforms’, *Energies*, vol. 11, no. 5, 2018, doi: 10.3390/en11051187.
[11] Y. Liu, S. Li, Q. Yi, and D. Chen, ‘Developments in semi-submersible floating foundations supporting wind turbines: A comprehensive review’, *Renew. Sustain. Energy Rev.*, vol. 60, pp. 433–449, 2016, doi: 10.1016/j.rser.2016.01.109.
[12] J. Taboada, ‘Comparative analysis review on Floating Offshore wind Foundations (FOWF)’, *Ing. Nav.*, no. 949, pp. 75–87, 2016.
[13] A. N. Robertson and J. M. Jonkman, ‘Loads analysis of several offshore floating wind turbine concepts’, in *Proceedings of the International Offshore and Polar Engineering Conference*, 2011, no. October, pp. 443–450.
[14] A. J. Goupee, B. J. Koo, R. W. Kimball, K. F. Lambrakos, and H. J. Dagher, ‘Experimental comparison of three floating wind turbine concepts’, *J. Offshore Mech. Arct. Eng.*, vol. 136, no. 2, pp. 1–10, 2014, doi: 10.1115/1.4025804.
[15] J. Chen, Z. Hu, and F. Duan, ‘Comparisons of dynamical characteristics of a 5 MW floating wind turbine supported by a spar-buoy and a semi-submersible using model testing methods’, *J. Renew. Sustain. Energy*, vol. 10, no. 5, 2018, doi: doi.org/10.1063/1.5048384.
[16] J. Jonkman, ‘Definition of the Floating System for Phase IV of OC3’, 2010.
[17] J. Jonkman, ‘Dynamics modeling and loads analysis of an offshore floating wind turbine, Ph.D. Thesis’, 2007.
[18] ANSYS, ‘AQWA Reference Manual Release 14.5’, Canonsburg, USA, 2012.
[19] J. M. Jonkman and M. L. Buhl Jr, ‘FAST user’s guide’, Golden, USA, 2005.
[20] National Renewable Energy Laboratory (NREL), ‘OpenFAST Documentation Release v3.0.0’, 2021.
[21] Y. Yang, ‘F2A User Manual’, 2020.
[22] Y. Yang, M. Bashir, C. Michailides, C. Li, and J. Wang, ‘Development and application of an aero-hydro-servo-elastic coupling framework for analysis of floating offshore wind turbines’, *Renew. Energy*, vol. 161, pp. 606–625, 2020, doi: 10.1016/j.renene.2020.07.134.
[23] B. J. Jonkman and M. L. Buhl Jr, ‘TurbSim User’s Guide - Technical Report NREL/TP-500-39797’, 2006.